Surface-structure libraries: multifrequential oscillations in catalytic hydrogen oxidation on rhodium

Citation for the original published paper (version of record):
Suchorski, Y., Datler, M., Bespalov, I. et al (2019). Surface-structure libraries: multifrequential oscillations in catalytic hydrogen oxidation on
rhodium. Journal of Physical Chemistry C, 123(7): 4217-4227.
http://dx.doi.org/10.1021/acs.jpcc.8b11421

THE JOURNAL OF PHYSICAL CHEMISTRY C

Article

Cite This: J. Phys. Chem. C 2019, 123, 4217−4227

pubs.acs.org/JPCC

Surface-Structure Libraries: Multifrequential Oscillations in Catalytic Hydrogen Oxidation on Rhodium

Yuri Suchorski,[†] Martin Datler,[†] Ivan Bespalov,[†,∥] Johannes Zeininger,[†] Michael Stöger-Pollach,[‡] Johannes Bernardi,[‡] Henrik Grönbeck,[§] and Günther Rupprechter*[,†]

[†]Institute of Materials Chemistry, Technische Universität Wien, Getreidemarkt 9, 1060 Vienna, Austria

[‡]USTEM, Technische Universität Wien, Wiedner Hauptstrasse 8-10, 1040 Vienna, Austria

[§]Department of Physics and Competence Centre for Catalysis, Chalmers University of Technology, 41296 Gothenburg, Sweden

ABSTRACT: Multifrequential oscillating spatiotemporal patterns in the catalytic hydrogen oxidation on rhodium have been observed in situ in the 10^{-6} mbar pressure range using photoemission electron microscopy. The effect is manifested by periodic chemical waves, which travel over the polycrystalline Rh surface and change their oscillation frequency while crossing boundaries between different Rh(*hkl*) domains. Each crystallographically specific μm-sized Rh(*hkl*) domain exhibits an individual wave pattern and oscillation frequency, despite the global diffusional coupling of the surface reaction, altogether creating a structure library. This unique reaction behavior is attributed to the ability of stepped surfaces of high-Miller-index domains to facilitate the formation of subsurface oxygen, serving as a feedback mechanism of kinetic oscillations. Formation of a network of subsurface oxygen as a result of colliding reaction fronts was observed in situ. Microkinetic model analysis was used to rationalize the observed effects and to reveal the relation between the barriers for surface oxidation and oscillation frequency. Structural limits of the oscillations, the existence range of oscillations, as well as the effect of varying hydrogen pressure are demonstrated.

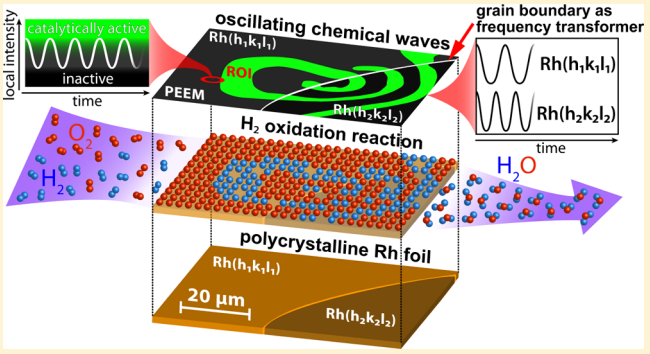

1. INTRODUCTION

Catalytic hydrogen oxidation has been intensively studied since the times of Döbereiner (1823) and Faraday (1834).[1−3] As CO oxidation, it is a prototypical surface reaction which initiated research in catalysis and contributed to the introduction of the term "catalysis" by Berzelius.[4] Significant experimental and theoretical efforts over the last 30 years have resolved the intermediate reaction steps[5−9] and shed light on the accompanying spatiotemporal effects from the nm- to the μm-scale.[10,11]

Nevertheless, the formation of water by oxidation of hydrogen on noble and other transition metals remains a complex reaction with many interesting and still unexplored features. Particularly, in view of solid state electrochemistry (fuel cells) and corrosion, the reaction remains an important research topic. Using the surface science approach to catalysis, hydrogen oxidation has been studied at high vacuum conditions on different single crystal surfaces of Pt, Pd, and Rh, revealing its pronounced surface-structure sensitivity.[6−16] However, only very few studies compared the reaction on different crystallographic orientations under the same experimental conditions. This is true for low Miller indices; not even speaking about highly stepped surfaces, as such studies would be very demanding and time-consuming from an experimental point of view. Surface-structure libraries[17] may be helpful in this case, as will be discussed in detail below.

The oscillating mode of the hydrogen oxidation reaction plays a particular role: under specific conditions, the reaction rate varies periodically, despite constant external parameters (gas pressures, temperature, and flow). Such self-sustained oscillations in heterogeneous catalytic reactions were first reported in the 1970s for CO oxidation on Pt,[18] and in the 1980s for NO reduction.[19] To date, the main body of work on oscillating surface reactions is still related to CO oxidation[20−22] and NO reduction,[23,24] predominately on single crystals of Pt group metals. The importance of oscillating surface reactions for catalysis was reflected by the Nobel Prize to Ertl in 2007.

In case of H_2 oxidation, self-sustained oscillations were observed on polycrystalline Pt and Pd wires,[25,26] polycrystalline Pt layers,[27] or supported Pd and Rh catalysts[28,29] under atmospheric pressure conditions. Under high vacuum conditions, oscillations in H_2 oxidation have been observed only on well-ordered bimetallic Rh/Ni surface alloys[30] and on sharp Rh nanotips under high electric field conditions (>10 V/nm).[31] In the latter case, the applied field causes oscillations by stimulating the periodic formation and reduction of Rh surface oxide. However, the oscillatory mode of catalytic H_2 oxidation

Received: November 26, 2018
Revised: January 18, 2019
Published: January 23, 2019

has not yet been observed under field-free conditions over single crystal surfaces of pure Rh.

In a recent short communication, we reported our first observation of multifrequential oscillations in the catalytic hydrogen oxidation on a polycrystalline Rh foil.[32] Apart from observing self-sustained oscillations in H_2 oxidation on the polycrystalline Rh surface, it was surprising that the reaction simultaneously oscillated with different frequencies on adjacent Rh(*hkl*) domains of differing crystallographic structures. The local frequency was related to the local crystallography: the more stepped the surface was, the higher was the observed frequency. This is quite unusual because although the crystalline grains forming the surface domains were separated by grain boundaries, they were well permeable for the hydrogen fronts traveling across the surface during the kinetic transitions.[33]

In the present contribution, we deepen and extend the obtained insights by focusing on the feedback mechanism and discussing structural limits of the observed effect. In situ monitoring of the reaction on individual domains of a polycrystalline Rh surface by photoemission electron microscopy (PEEM) provides strong indications that the structure-sensitive subsurface oxygen formation serves as the feedback mechanism. A mean-field microkinetic modelling further rationalizes the experimental results and explains the experimentally observed structural limits.

2. EXPERIMENTS

2.1. Hydrogen Oxidation in a μm-Sized Confined Reaction System. Initially, the present study aimed at the generation of oscillations in H_2 oxidation on a Rh(1 1 1) single crystal surface. Experiments were performed in a multipurpose ultra-high vacuum (UHV) apparatus consisting of separate PEEM and X-ray photoelectron spectroscopy (XPS) chambers. The XPS chamber for examination of surface composition was connected to the PEEM chamber by a sample transfer line, allowing fast transfer without breaking UHV. The PEEM chamber was used as a flow reactor in which the Rh surface was exposed to molecular oxygen and hydrogen in the 10^{-6} mbar pressure range. A 10 × 10 mm^2 [1 1 1]-oriented Rh single crystal (Mateck, 99%) was used as a sample. After repeated standard UHV cleaning procedures (Ar^+ sputtering and annealing), the surface cleanliness was confirmed by XPS before each single reaction measurement. The sample temperature was measured by a Ni/NiCr thermocouple spot-welded directly to the sample. The reactant gases (O_2 and H_2) were dosed by precision leak valves and the reaction product H_2O was continuously pumped off by a turbomolecular pump.

Despite exploring an extended range of partial pressures (10^{-5} to 10^{-7} mbar) and temperatures (373−573 K), it was not possible to generate an oscillating mode of hydrogen oxidation on the smooth Rh(1 1 1) surface. However, periodically alternating patterns of different PEEM brightnesses were detected in a μm-sized furrow-like defect (scratch) on the Rh(1 1 1) surface upon exposure to an O_2/H_2 gas phase with constant partial pressures of $p_{O_2} = 1.1 \times 10^{-6}$ mbar, $p_{H_2} = 8.4 \times 10^{-7}$ mbar, at constant $T = 433$ K. Figure 1 illustrates the observed effect, demonstrating both the spatial and temporal periodicity (left and right inset in Figure 1a, respectively) of the PEEM image intensity. In the Figure 1b local PEEM intensities registered in the different regions of interest (ROIs) inside and outside the furrow are compared.

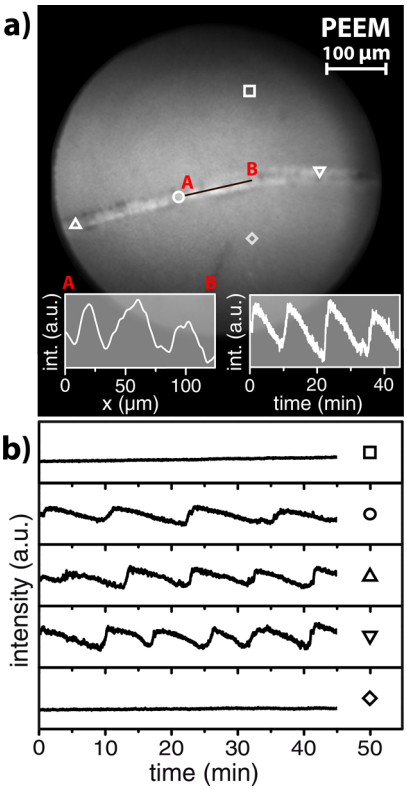

Figure 1. Oscillations in H_2 oxidation confined in a furrow-like defect on a Rh(1 1 1) surface: (a) PEEM video frame of ongoing H_2 oxidation, with the smooth Rh(1 1 1) surface being in an inactive steady state, whereas pulse-like oscillations occur inside the furrow. White geometrical symbols mark the position of the ROIs. The left hand inset illustrates the periodicity in space for the area A → B along the furrow, whereas the right hand inset demonstrates the periodicity in time measured for the ROI marked by a circle; (b) local PEEM intensity registered within the furrow (○, Δ, ▽), compared to those on the smooth Rh surface (□ and ◊). Part (b) is adapted from ref 32 (Copyright 2018, Springer Nature).

The occurrence of spatially periodical patterns, which also exhibit temporal periodicity, is characteristic for "propagating waves" during oscillating surface reactions.[20−22,34,35] Because the local PEEM image intensity is related to the local work function[36] and the latter correlates with the surface coverage of reactants,[37] Figure 1 proves that the observed waves consist of concentration gradients of adsorbed hydrogen and oxygen. Accordingly, Figure 1 shows an oscillating hydrogen oxidation reaction, a reaction mode, which had not yet been observed on a Rh(1 1 1) surface (and also not on any other pure Rh single crystal surface).

To understand the observed phenomenon, the morphology and surface structure of the μm-sized furrow were studied in detail by electron back-scatter diffraction (EBSD) and atomic force microscopy (AFM). The EBSD measurements were performed using a field emission scanning electron microscope (SEM FEI Quanta 200F), applying standard EBSD conditions and evaluation procedures.[38] The AFM measurements were carried out by employing the AFSEM (GETec Microscopy, Austria), integrated with the SEM. The design allows simultaneous operation of SEM and AFM, the latter being installed in the SEM vacuum chamber, thus providing correlated crystallographic and topological information, respectively.

DOI: 10.1021/acs.jpcc.8b11421
J. Phys. Chem. C 2019, 123, 4217−4227

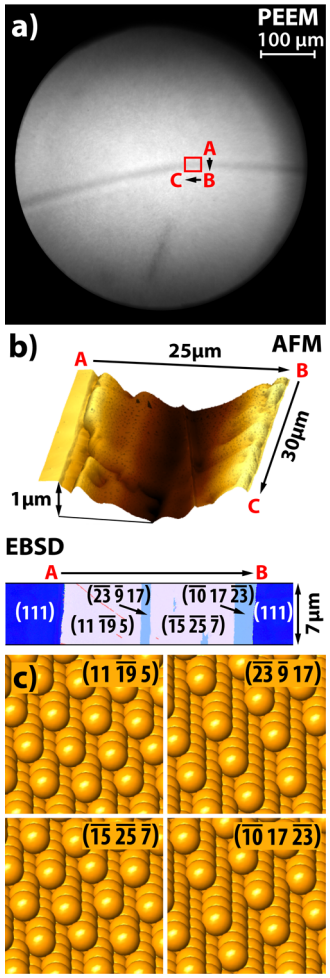

Figure 2. Micrometer-sized furrow on a Rh(1 1 1) surface acts as the confined reaction system: (a) PEEM image of the Rh(1 1 1) single crystal surface containing a furrow-like defect (indentation), the region where EBSD and AFM measurements were performed is marked; (b) example of the profile of the furrow, as imaged by AFM, the lower inset shows the EBSD color-coded map (7×35 μm^2) of a typical region of the furrow with the Miller indices indicated; and (c) ball models of stepped structures present on the walls of the furrow.

Figure 2 shows the PEEM image of the Rh(1 1 1) surface, including the defect where oscillations were found, and an exemplary AFM profile and EBSD map of the surface region marked in Figure 2a. Ball models of some typical surface structures of the furrow walls are shown in Figure 2c.

The main property differentiating the smooth Rh(1 1 1) surface from the surface inside the furrow, where the oscillations were observed, is the surface roughness. The furrow walls consist of highly stepped and kinked surfaces (cf. EBSD in Figure 2b and corresponding structure models in Figure 2c). Apparently, such highly corrugated surfaces are required to generate oscillations in H_2 oxidation on Rh.

Figure 1b demonstrates that the frequency of oscillations varies along the furrow, suggesting that the degree of atomic roughness/corrugation governs the oscillations. This explains why the atomically smooth Rh(1 1 1) surface does not exhibit oscillations and why the μm-sized rough furrow serves as a mesoscopically confined reaction system. Note also that the oscillations do not "spill over" to the adjacent flat Rh(1 1 1) surface. To shed more light on the observed oscillations, a systematic study using different highly corrugated (i.e., stepped and kinked) Rh surfaces is required. Usually, such studies are performed by sequentially (i.e., one after the other) using differently oriented high-Miller-index single crystals, which would be quite time-consuming. Furthermore, for a true quantitative comparison of different single crystals, identical reactant pressures, identical temperatures, and identical temperature ramps are required, placing high demands on experiments.

An alternative approach is to generate a "surface-structure library", that is, to construct a sample containing adjacent regions of different highly stepped crystallographic orientation. Then, the catalytic behavior of different regions can be directly compared, provided that spatial coupling between the regions is effectively inhibited.[39]

During the present experiments, all the different regions are "automatically" exposed to the same pressure and temperature conditions, but the determination of specific (local) catalytic properties requires spatially resolved surface analysis methods. As already mentioned, polycrystalline metal foils which consist of many μm-sized, crystallographically differently oriented (*hkl*)-domains separated by grain boundaries, provide a possibility for surface-structure libraries.[17] Applying the local *kinetics by imaging* approach with PEEM as imaging tool, the details of the reaction process on individual μm-sized domains can be studied.[40,41]

Such surface-structure libraries, based on polycrystalline Pt and Pd foils, have already been successfully used for a direct comparison of the CO oxidation properties of various Pt(*hkl*) and Pd(*hkl*) surfaces.[39,41,42] The surface diffusion coupling, which would disturb the independent behavior of individual domains, was effectively inhibited by grain boundaries and the gas phase coupling was negligible in the 10^{-6} mbar pressure range, at least for CO oxidation.[39] It seems promising to apply such a surface-structure library approach to H_2 oxidation on Rh.

2.2. Self-Sustained Oscillations on a Polycrystalline Rh Surface. A polycrystalline Rh foil exhibits many crystallographically differently oriented μm-sized domains, which are separated by grain boundaries (Figure 3a). The crystallographic orientation of the individual domains was determined by EBSD (Figure 3b) and because the individual domains are in the 10−300 μm size range, a range of different orientations can be found on such a sample (Figure 3c). A proper set of interesting orientations (e.g., stepped/kinked surfaces) can then be selected and the ongoing reaction can be monitored simultaneously on several well-defined domains (Figure 4).

Again, the PEEM chamber was used as a flow reactor and after an induction period at constant O_2/H_2 ($p_{O_2} = 1.1 \times 10^{-6}$ mbar, $p_{H_2} = 8.4 \times 10^{-7}$ mbar, and $T = 433$ K) a complex turbulence-like "living" surface appeared during ongoing H_2 oxidation, consisting of repeatedly nucleating spirals (Figure 4b). The spirals spread across the domains and overlapped at the domain boundaries, creating complex "stirring" patterns. Note that the rotation speed of the spirals strongly varied for different surface orientations.

The dark areas correspond to the oxygen-covered inactive surface, and bright zones to the catalytically active oxygen-deficient surface with low hydrogen coverage.[43] The picture in Figure 4b thus shows a snapshot of concentration waves moving across the surface. To exemplify this motion, the position of an arbitrarily selected wave crest is traced in Figure 4c−f. In similarity with the furrow on Rh(1 1 1), both

DOI: 10.1021/acs.jpcc.8b11421
J. Phys. Chem. C 2019, 123, 4217−4227

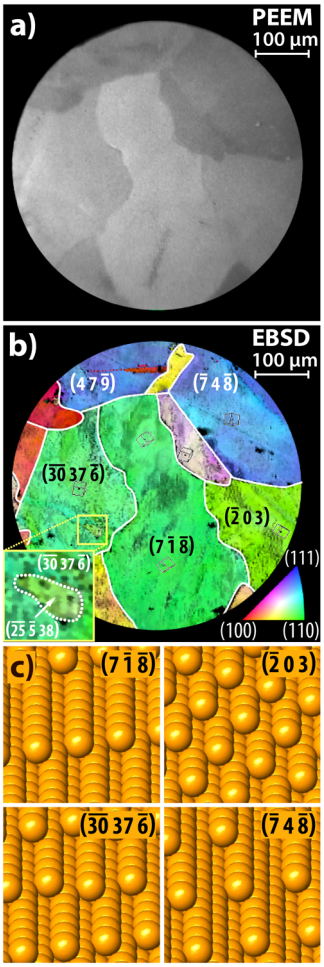

Figure 3. Polycrystalline Rh foil as the surface-structure library: (a) PEEM image of clean Rh foil consisting of μm-sized differently oriented high-Miller-index domains (field of view 520 μm); (b) EBSD color-coded map of the same region with crystallographic orientations indicated. The inverse pole figure is shown for reference in the bottom right corner. A magnified view of a 45 × 45 μm^2 region with a crystallographic $(\bar{2}\bar{5}\ \bar{5}\ 38)$ orientation within the $(\bar{3}0\ 37\ \bar{6})$ domain is shown as inset; (c) ball models of different stepped structures, visible in the field of view of (a) and identified in (b). Adapted in part from ref 33 (Copyright 2016, Springer Nature).

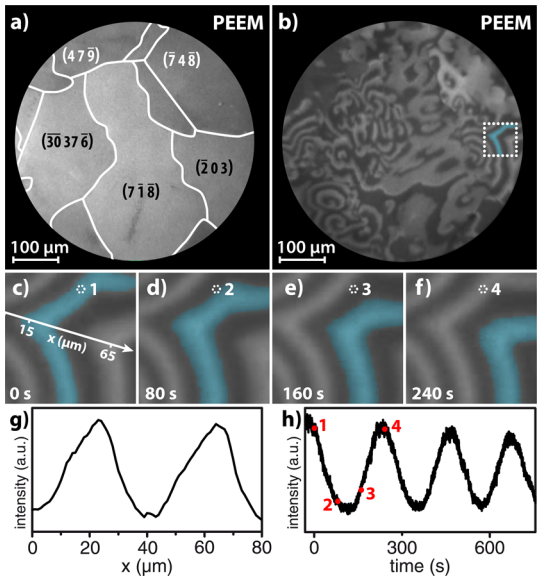

Figure 4. Oscillating H_2 oxidation on polycrystalline Rh: (a) PEEM image of the clean Rh surface, grain boundaries, and Miller indices are marked (cf. Figure 3b); (b) PEEM snapshot of the same area during the ongoing reaction; the marked rectangular region is magnified in (c–f); (c–f) illustration of the propagation of a chemical wave, an arbitrarily selected wave crest is colored blue; (g) momentary distribution of the local PEEM intensity along the *x*-axis in (c) illustrating spatial periodicity; (h) time dependence of the local PEEM intensity at the circular ROI marked in (c–f) illustrating temporal periodicity. The time points corresponding to the particular frames are marked with "1" to "4" in (h). $p_{O_2} = 1.1 \times 10^{-6}$ mbar, $p_{H_2} = 8.4 \times 10^{-7}$ mbar, and $T = 433$ K. Adapted in part from ref 32 (Copyright 2018, Springer Nature).

necessary attributes of a wave process are present, namely, spatial and temporal periodicity, as shown in Figure 4g,h.

The digitally recorded PEEM video sequences were analyzed pixel-by-pixel using differently sized and shaped ROIs, which can be arbitrarily placed at any position within the field of view, like "virtual probe holes". The image brightness analysis revealed differing local oscillation frequencies for different surface domains, as illustrated in Figure 5a, in which the observed local oscillation frequencies are displayed as a "frequency map". Because the crystallographic orientation of the individual domains is known from EBSD, the local oscillation frequencies can be correlated with the local surface structure of the corresponding domains (Figure 5b).

The main result of the data compendium in Figure 5 is that the local oscillation frequencies clearly correlate with the local surface structure: the more stepped (more rough) the surface is, the higher the observed frequency. In Figure 5b, the atomic scale roughness increases in the order of ROI 1–4 and so does the frequency. This explains why, despite extended efforts, oscillating H_2 oxidation was never observed on flat Rh surfaces, such as Rh(1 1 1), under high-vacuum conditions (also upon significantly varying p_{O_2}, p_{H_2} and T). To establish a quantitative correlation between the frequency and surface roughness is difficult, however, due to the unknown weighting of several contributions, for example, step density, kink atom density, and width and orientation of terraces, to the feedback process (see chapter 2.3 below).

Reports about field-induced oscillations on nm-sized Rh tips[44] also fit well into this picture because such tips mainly consist of highly stepped surfaces in between the small facets, many of them are also stepped.[45] Apparently, as in the case of the furrow on the Rh(1 1 1) surface, a certain degree of surface roughness is required to generate oscillations. The clear correlation between the structure of particular domains on the polycrystalline surface and the observed oscillation frequency suggests that a structure-sensitive feedback mechanism may exist, linking the local structure to the adsorption and reaction kinetics and thus governing the observed oscillations.

2.3. Indications for the Feedback Mechanism. Similar as oscillations in electric control circuits, self-sustained oscillations in chemical systems need a feedback loop for maintaining their existence.[46] Different surface processes have been reported as feedback mechanisms in heterogeneous catalytic systems: structural phase transitions of the catalyst surface, faceting or formation of surface protrusions, and oxidation and reduction processes.[21,22,24,47,48] The relatively long periods of the current oscillations (on the order of minutes) suggest that a slow surface process causes transitions

DOI: 10.1021/acs.jpcc.8b11421
J. Phys. Chem. C 2019, 123, 4217–4227

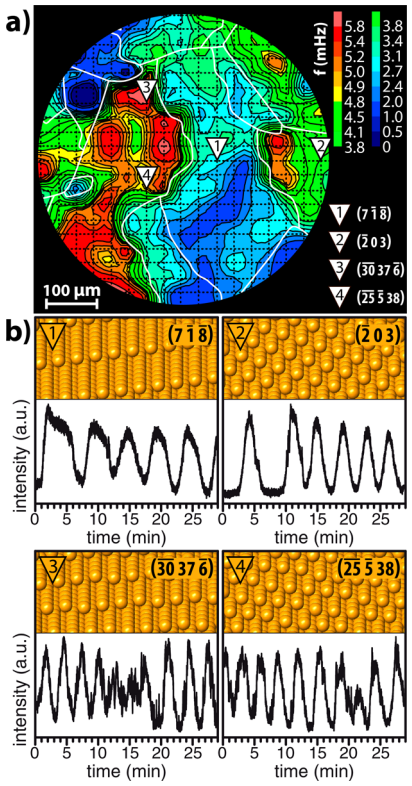

Figure 5. Multifrequential oscillations in hydrogen oxidation on polycrystalline Rh at constant $p_{O_2} = 1.1 \times 10^{-6}$ mbar, $p_{H_2} = 8.4 \times 10^{-7}$ mbar, and T = 433 K: (a) "frequency map" of the observed oscillations. Crystallographically different domains are marked with white lines and the Miller indices determined by EBSD are indicated on the right side (cf. EBSD map in Figure 3b); (b) time dependence of local PEEM intensity of four selected regions. The positions of the corresponding circular ROIs (of 1 μm diameter) are located in the centers of the numbered triangular symbols in (a). The ball model insets illustrate the stepped surface structure of the selected regions, (a) adapted in part from ref 32 (Copyright 2018, Springer Nature).

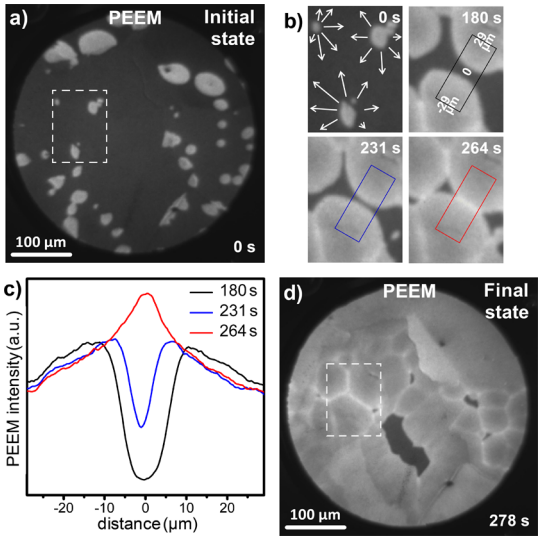

Figure 6. Formation of a low work function network due to collisions of hydrogen reaction fronts in H_2 oxidation on polycrystalline Rh foil: (a) PEEM-video frame showing the active (bright) surface nucleating on the inactive (dark) surface of polycrystalline Rh foil at $p_{O_2} = 7.7 \times 10^{-7}$ mbar, $p_{H_2} = 1 \times 10^{-6}$ mbar, and 513 K; (b) collision of reaction fronts nucleating within the rectangular region marked in (a). The collisions lead to the formation of regions of low work function on the surface and corresponding bright stripes in the PEEM image; (c) intensity profiles measured within the three color-coded areas marked in (b); (d) network structure remaining after collisions of hydrogen fronts.

between the active and inactive state and vice versa. Oxidation/reduction of the substrate surface seems to be most probable for such slow process. The essential role of the stepped Rh surface, the fact that oscillating H_2 oxidation does not occur on smooth low index Rh surfaces, and the structural limits discussed below, suggest a periodical formation and depletion of subsurface oxygen as the present feedback mechanism. An alternative feedback mechanism based on surface reconstruction, known from oscillating CO oxidation on some Pd and Pt single-crystal surfaces,[21,22,24,47,49] is highly unlikely here, because it can hardly be expected that dozens of differently oriented Rh domains would simultaneously exhibit similar reconstructions, but with different frequencies.

Additional support for such a subsurface oxygen feedback mechanism can be derived from the observation of colliding reaction fronts in the bistable regime of H_2 oxidation on polycrystalline Rh. Figure 6 shows an isothermal kinetic transition from the inactive steady state (oxygen covered Rh surface, dark PEEM contrast) to the catalytically active (reduced surface, bright PEEM contrast) at a constant temperature of 513 K. Islands of the active surface (bright areas in Figure 6a) nucleate at surface defects and the reaction fronts (forming island borders) spread at the expense of the inactive (dark) surface. Consecutive PEEM snapshots in Figure 6b and the local PEEM intensity profiles (Figure 6c) illustrate what happens when hydrogen fronts approach each other and collide. The "collision line" appears much brighter than the active surface behind the fronts, demonstrating the formation of low work function areas where the fronts collide. A similar behavior has been observed earlier in catalytic CO oxidation on Pt(1 0 0) and (1 1 0),[50,51] in the nonoscillatory H_2 oxidation on Rh(1 1 1)[15,16] and in catalytic NO reduction on Rh(1 1 1).[52] In all these studies, areas of low work function have been associated to subsurface oxygen formation, as corroborated by model calculations.[16] A mechanism was proposed, in which coadsorbed hydrogen facilitates the formation of subsurface oxygen by lowering the activation barrier for oxygen diffusion through the metal surface.[16] Atomic hydrogen rapidly diffusing away from approaching reaction fronts increases the local hydrogen coverage on the still-oxygen covered surface between the fronts. Such artificially enhanced H + O coadsorption may lead to distortions of the substrate lattice, thus lowering the activation barrier of oxygen subsurface diffusion.

This proposed mechanism is in agreement with the present observations: after collision and annihilation of hydrogen fronts, a bright network of "collisions stripes" remains on the surface, that is, a landscape of the enhanced subsurface oxygen population (Figure 6d). It is important to note that the stripes do not coincide with the grain boundaries (cf. Figure 4a).

Apparently, the surface lattice is restored immediately after the collision of fronts, forming a "trap" for the oxygen atoms stored under the surface. Thus, the depletion of the oxygen reservoir is much slower than its formation.

Because the observed oscillation frequencies differ on differently oriented Rh domains, the proposed feedback

DOI: 10.1021/acs.jpcc.8b11421
J. Phys. Chem. C 2019, 123, 4217−4227

mechanism must be structure dependent. Indeed, structure dependence is expected for subsurface oxygen formation because the activation energy of oxygen penetration through the metal surface depends in a straightforward manner on the surface structure.[53,54] The formation of subsurface oxygen not only governs the generation but also the propagation of chemical waves. Waves crossing the grain boundaries may abruptly change their shape, the propagation velocity, and frequency of the oscillation. This is demonstrated in Figure 7,

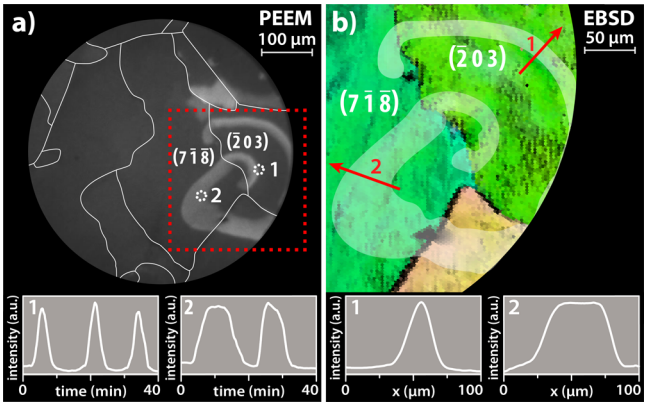

Figure 7. Effects of the grain boundary: (a) a spiral-shaped concentration wave propagating across the grain boundary between two differently structured domains during H_2 oxidation on Rh (p_{O_2} = 7.7 × 10^{-7} mbar, p_{H_2} = 5.5 × 10^{-7} mbar, and T = 433 K). The insets 1 and 2 show the temporal progression of the local PEEM intensity registered at two circular ROIs placed on the Rh(2̄ 0 3) and Rh(7 1̄ 8̄) domains, respectively; (b) EBSD map of the rectangular region marked by red dotted line in (a) with the overlapped spiral wave. The insets 1 and 2 show the local PEEM intensity profiles across the propagating waves (as marked with red arrows) on the Rh(2̄ 0 3) and Rh(7 1̄ 8̄) domains, respectively.

which presents the PEEM image and properties of a single spiral-shaped wave generated on a defect within the Rh(2̄ 0 3) domain, which propagates across the grain boundary and across the adjacent Rh(7 1̄ 8̄) domain. The insets in Figure 7a illustrate the frequency changes, whereas the local PEEM intensity profiles in Figure 7b illustrate changes in the shape of the propagating wave.

Such abrupt changes at the grain boundary demonstrate that oscillations reflect the properties of the particular Rh(*hkl*) domain and its behavior is not affected by neighbouring domains. This can be understood when one considers subsurface oxygen formation as the feedback mechanism. The rate of formation and of depletion of subsurface oxygen and thus the frequency *strictly* depends on the surface structure of the "oscillating" domain and cannot be influenced "from the outside", that is, by the surrounding domains. Therefore, the frequency changes abruptly at the grain boundary. In turn, the shape and "wavelength" also depend on the diffusion/reaction coupling within the propagation phase, whereas the surface structure contributes via its influence on the diffusion and reaction rate. For the almost terrace-free Rh(2̄ 0 3) surface (cf. Figure 5b), PEEM videos indicate that the propagation velocity is nearly isotropic, whereas an anisotropic front propagation is observed on the Rh(7 1̄ 8̄) surface. This surface consists of extended terraces (cf. Figure 3c) on which the fronts move with almost double velocity along the steps, compared to that across the steps. This results in a significantly modified shape and "wavelength" of propagating chemical waves. In principle, this effect shows a certain (purely outward) similarity to the change in light wavelength upon change of the refractive index in an anisotropic transition medium.

2.4. Structural Limitations of Oscillations. A detailed inspection of the recorded videoframes also revealed surface regions within the turbulent global picture, where the reaction did not oscillate, that is, the local PEEM intensity remained constant (Figure 8) despite diffusive coupling. Correlating

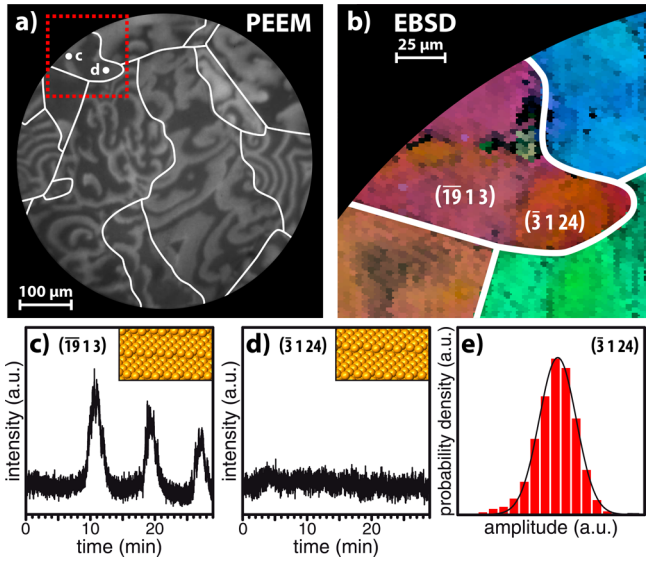

Figure 8. Structural limits in oscillating H_2 oxidation on polycrystalline Rh: (a) PEEM snapshot at constant p_{O_2} = 1.1 × 10^{-6} mbar, p_{H_2} = 8.4 × 10^{-7} mbar, and T = 433 K: (b) the EBSD map of the square region marked in (a). Two crystallographically different (1̄9 1 3) and (3̄ 1 24) structures were identified within the "red color" domain; (c,d) time dependences of local PEEM intensities for the (1̄9 1 3) and (3̄ 1 24) regions, respectively, the corresponding ROIs are marked in (a). The insets show the corresponding surface structures; (e) probability density distribution of the signal amplitude shown in (d).

PEEM videofiles with EBSD data identified such a non-oscillating region as the Rh(3̄ 1 24) structure within a ∼100 μm wide domain, where also the Rh(1̄9 1 3) structure was present without separation by a grain boundary (Figure 8b).

This finding was surprising because one would rather expect that nonoscillating regions were confined by grain boundaries. Apparently, the local structure dominates over coupling effects and certain surface structures exhibit activation energies for subsurface oxygen formation and reduction that under the present conditions are "too high". Given that subsurface oxygen formation indeed provides the feedback mechanism, these structural limits should depend on external parameters: for a given activation energy of subsurface oxygen formation, the rate of its formation is determined by the oxygen partial pressure and the temperature. Figure 9 confirms this hypothesis, by examining oscillations at conditions different from those in Figure 4, that is, at the same p_{O_2} = 1.1 × 10^{-6} mbar but higher p_{H_2} = 1.1 × 10^{-6} mbar. The oscillations on the Rh(2̄ 0 3) domain slow down (cf. Figure 4b) and the oscillations on the "less rough" Rh(7 1̄ 8̄) surface fully stop. Evaluation of other differently structured domains confirmed this trend that all evaluated facets exhibited lower frequencies than the corresponding ones in Figure 4.

DOI: 10.1021/acs.jpcc.8b11421
J. Phys. Chem. C 2019, 123, 4217−4227

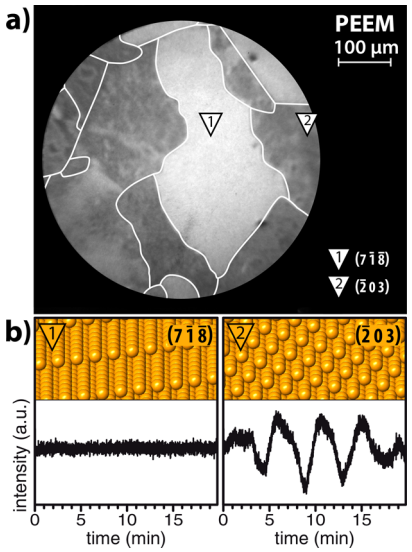

Figure 9. Structural limits for oscillations depend on the external parameters: (a) PEEM snapshot taken during oscillations in H_2 oxidation on polycrystalline Rh at $p_{O_2} = 1.1 \times 10^{-6}$ mbar, $p_{H_2} = 1.1 \times 10^{-6}$ mbar, and $T = 433$ K; (b) PEEM intensity locally recorded for Rh(7 $\bar{1}$ $\bar{8}$) and Rh ($\bar{2}$ 0 3) domains. Upper parts in (b) show the corresponding surface-structure ball models.

Similar as the front collision network discussed above, the parameter-dependent structural limits of the observed oscillations strongly support the hypothesis of the formation and depletion of subsurface oxygen being the feedback mechanism of self-sustained oscillations.

3. MICROKINETIC ANALYSIS

Using X-ray photoelectron diffraction, the formation of subsurface oxygen was directly observed for smooth Rh(1 1 1), at 470 K and oxygen exposures similar to the current experiments.[55] Although the PEEM/XPS setup used herein cannot provide direct evidence of subsurface oxygen, it is reasonable to assume that rough Rh surfaces might form Rh oxide structures at lower temperatures than Rh(1 1 1). To rationalize the suggested course of the oscillations and, in particular, to verify the feedback mechanism, the observed oscillations were analyzed by a mean-field micro-kinetic model based on the well-established Langmuir–Hinshelwood (LH) mechanism for H_2 oxidation on Rh.[56]

To account for the observed oscillations, the model by McEwen and co-authors, describing field-induced oscillations in H_2 oxidation on Rh,[44,57] was modified for a field-free case. In this model, the LH reaction network includes five steps which are schematically shown in Figure 10: the dissociative adsorption (and associative desorption) of hydrogen (R1), dissociative adsorption (and associative desorption) of oxygen via a precursor state (R2, R3), formation and reduction of subsurface oxygen (R4), and catalytic water formation (R5).

The partial coverages of hydrogen, oxygen, and subsurface oxygen (θ_H, θ_O, and θ_s, correspondingly) are expressed in the mean-field approach by the following rate equations

$$\frac{d\theta_H}{dt} = 2k_a^H p_{H_2} \theta_*^2 - 2k_d^H \theta_H^2 - 2k_r \theta_H \theta_O$$

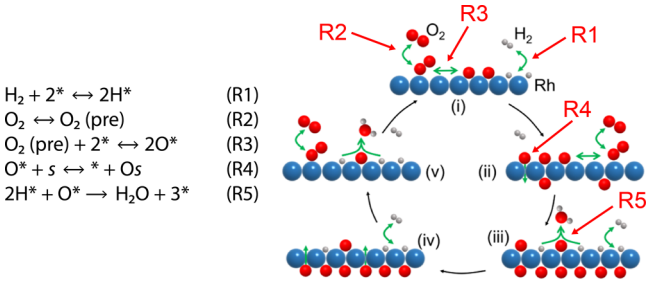

$H_2 + 2* \leftrightarrow 2H*$ (R1)
$O_2 \leftrightarrow O_2$ (pre) (R2)
O_2 (pre) $+ 2* \leftrightarrow 2O*$ (R3)
$O* + s \leftrightarrow * + Os$ (R4)
$2H* + O* \longrightarrow H_2O + 3*$ (R5)

Figure 10. Reaction equations and schematic representation of the reaction steps in H_2 oxidation on Rh. Color code: Rh (blue), O (red), and H (gray). In R1–R5, * and s correspond to empty surface and subsurface sites, respectively.

$$\frac{d\theta_O}{dt} = \frac{2}{1 + K\theta_*^2}(k_a^O K p_{O_2} \theta_*^2 - k_d^O \theta_O^2) - k_{ox}\theta_O(1 - \theta_s) + k_{red}\theta_s\theta_* - k_r\theta_H\theta_O$$

$$\frac{d\theta_s}{dt} = k_{ox}\theta_O(1 - \theta_s) - k_{red}\theta_s\theta_*$$

The empty sites are given by $\theta_* = 1 - \theta_H - \theta_O$ and the rate constants are given by

$$k_A^H = S_0^H a_s / \sqrt{2\pi m_{H_2} k_B T}$$

$$k_a^O = S_0^O a_s / \sqrt{2\pi m_{O_2} k_B T}$$

$$k_d^H = k_{d0}^H e^{-\beta E_d^H}$$

$$K = K_0 e^{-\beta(E_K + A_K^O \theta_O + A_K^s \theta_s)}$$

$$k_d^O = k_{d0}^O e^{-\beta(E_d^O + A_d^O \theta_O + B_d^O \theta_O^2)}$$

$$k_{ox} = k_{ox}^0 e^{-\beta E_{ox}}$$

$$k_{red} = k_{red}^0 e^{-\beta(E_{red} + A_{red}^s \theta_s)}$$

$$k_r = k_r^0 e^{-\beta(E_r + A_r^H \theta_H + A_r^O \theta_O)}$$

The molecular masses are given by m_{H_2} and m_{O_2}, S_0^X denotes the initial sticking probabilities and a_s is the area of a surface site (10 Å^2); $\beta = 1/k_B T$.

The values of the kinetic parameters used are listed in Table 1. The values are those previously determined for Rh(1 1 1),[44] except the activation energies of oxide formation and reduction and the sticking coefficient of hydrogen.

In refs,[44,57] to mimic the field-induced oscillations, a hydrogen sticking coefficient of 0.3 was used. For the current field-free reaction, a slightly higher sticking coefficient of 0.4 is required to obtain oscillations (while keeping the other parameters constant). The simulations were performed for 433 K, which is much higher than the water desorption temperature on Rh(0 0 1)[58] of 300 K. One can thus safely assume that the formed water immediately desorbs, especially because the UHV PEEM chamber was operated as a "flow reactor", which was continuously pumped off, preventing readsorption of water.

The surface oxidation was modeled as a single step. This is apparently a simplification, as the elementary steps of oxidation/reduction may be complex, including significant

DOI: 10.1021/acs.jpcc.8b11421
J. Phys. Chem. C 2019, 123, 4217–4227

Table 1. Model Parameters

symbol	description	value
E_d^H	desorption energy of H	0.70 eV
S_0^O	initial sticking coefficient O	0.60
A_K^s	coverage dependence of sub-surface oxygen on oxygen dissociation	0.082 eV
E_{ox}	activation energy for oxygen diffusion from surface to sub-surface sites	1.111 eV
E_d^O	desorption energy of O	2.85 eV
A_d^O	coverage dependence of oxygen desorption energy on adsorbed oxygen	−0.4 eV
B_d^O	coverage dependence of oxygen desorption energy on molecular oxygen	−0.5 eV
E_r	activation energy for water formation	0.75 eV
s_0^H	initial sticking coefficient H	0.4
k_{d0}^H	pre-factor	3.0×10^{10} s^{-1}
K^0	pre-factor	0.2525 s^{-1}
E_K	activation energy	−0.178 eV
A_K^O	coverage dependence of adsorbed oxygen on oxygen dissociation	0.158 eV
k_{ox}^0	pre-factor	5.0×10^{11} s^{-1}
k_{red}^0	pre-factor	1.85×10^{13} s^{-1}
A_{red}^s	coverage dependence of sub-surface oxygen on surface subsurface reduction	0.3 eV
k_{d0}^O	pre-factor	6.0×10^{13} s^{-1}
k_r	pre-factor	7.0×10^{12} s^{-1}
A_r^H	coverage dependence of activation energy of H_2O formation on H	−0.27 eV
A_r^O	coverage dependence of activation energy of H_2O formation on O	−0.145 eV

structural rearrangements.[57] However, as the exact activation energies are unknown for the considered high-index Rh surfaces, we resort to one effective barrier. This barrier should be regarded an apparent energy barrier, rather than reflecting a single elementary step. Furthermore, it is reasonable that the oxidation and reduction processes are coupled, assuming a linear relation between E_{ox} and E_{red} as suggested by the data in ref 56

$$E_{red} = 0.293 + 0.776E_{ox}$$

E_{ox} for Rh(1 1 1) was reported to be 1.68 eV.[57] From experiments, it is known that oscillations do not occur on Rh(1 1 1), indicating that 1.68 eV is too high to enable self-sustained oscillations in the field-free case. However, experiments have shown that the oxidation of Rh(1 1 1) proceeds rather via surface steps than through the metal layer and that the rate depends on the direction of the oxidation.[59] For the stepped Rh surfaces studied herein, it is reasonable to assume that oxides form more readily, as the required atomic rearrangements are easier for low-coordinated surface sites. Keeping other parameters constant, we obtain oscillations with E_{ox} in the range 1.021−1.161 eV at a temperature of 433 K and hydrogen and oxygen pressures of 0.84×10^{-6} mbar 1.1×10^{-6} mbar, respectively. We note that, within the span of E_{ox} that yields oscillations, E_{red} is larger than E_{ox}. This agrees with the experimental observation that the depletion of the oxygen reservoir is slower than its formation. The calculated effect of hydrogen pressure on the oscillations is shown in Figure 11: with E_{ox} = 1.111 eV, the frequency is 5.7×10^{-3} s^{-1} for $p_{H_2} = 0.84 \times 10^{-6}$ mbar and increases to 6.7×10^{-3} s^{-1} for $p_{H_2} = 0.90 \times 10^{-6}$ mbar. Similarly, lowering the hydrogen pressure makes the oscillation frequency smaller (not shown).

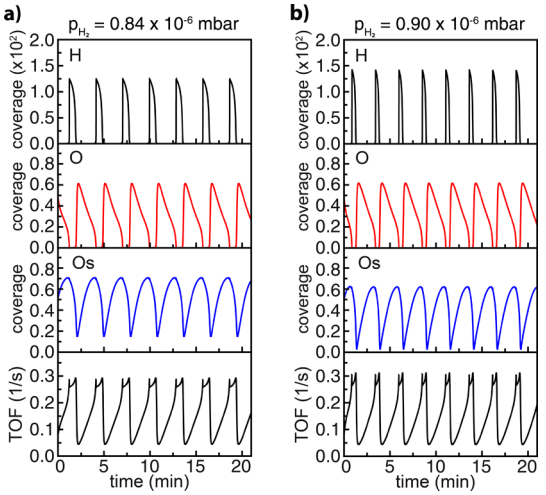

Figure 11. Oscillation in H_2 oxidation on Rh. Top to bottom panels show the coverage of hydrogen (H), of oxygen (O), of subsurface oxygen (Os) and the reaction rate as turnover frequency (TOF). The simulations have been performed at T = 433 K and partial pressures of oxygen and hydrogen of (a) 1.1×10^{-6} mbar and 0.84×10^{-6} mbar and (b) 1.1×10^{-6} mbar and 0.90×10^{-6} mbar, respectively. E_{ox} was set to 1.111 eV.

The surface processes are affected, besides the external conditions, also by several parameters in the model: by energies of adsorption, desorption, and reaction in a direct way and indirectly by the coverage dependences. Because it is unknown how these parameters change for the differently oriented domains we concentrated on variations of the E_{ox}/E_{red} parameter to explore the model.

Figure 12 illustrates the role of this parameter: Figure 12a shows the dependence of the oscillation frequency on E_{ox} for two hydrogen pressures, 0.84×10^{-6} mbar and 0.90×10^{-6} mbar, respectively, and Figure 12b displays the resulting

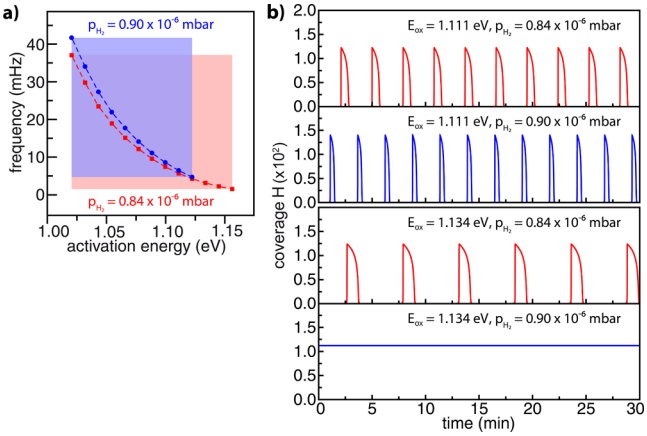

Figure 12. Sensitivity of oscillations to the activation energy of subsurface oxygen formation: (a) dependence of the oscillation frequency on E_{ox} for $p_{H_2} = 0.84 \times 10^{-6}$ mbar (red curve) and for $p_{H_2} = 0.90 \times 10^{-6}$ mbar (blue curve). Red and blue areas mark the existence range of oscillations for p_{H_2} of 0.84×10^{-6} mbar and 0.90×10^{-6} mbar, correspondingly; (b) H coverage as function of time for E_{ox} = 1.111 eV, $p_{H_2} = 0.84 \times 10^{-6}$ mbar and $p_{H_2} = 0.90 \times 10^{-6}$ mbar (upper two panels) and for E_{ox} = 1.134 eV and the same p_{H_2} values (lower two panels).

DOI: 10.1021/acs.jpcc.8b11421
J. Phys. Chem. C 2019, 123, 4217−4227

oscillations. The results in Figure 12 confirm that the observed oscillations sensitively depend on the rate of subsurface oxygen formation and its depletion, both governed by the activation energy E_{ox}.

At p_{H_2} of 0.84×10^{-6} mbar, the calculated oscillation frequency is 2.7×10^{-3} s^{-1} for an E_{ox} value of 1.021 eV, whereas it is only half (1.4×10^{-3} s^{-1}) for E_{ox} of 1.161 eV. Thus, the easier the subsurface oxygen is formed, the higher is the oscillation frequency. This agrees well with the experiments, as a higher frequency was observed for highly stepped surfaces. Similarly, when the activation energy for Rh surface oxidation was lowered by a high electric field, oscillations occurred on Rh nanotips even under high-vacuum conditions.[44,57]

The role of E_{ox} is clear when considered together with pressure variation: at E_{ox} of 1.111 eV, a pressure increase from 0.84×10^{-6} mbar to 0.90×10^{-6} mbar leads solely to a frequency increase. In turn, for a surface with minimally higher E_{ox} of 1.134 eV, the same pressure increase moves the surface out of the phase space for oscillations, making the oscillations disappear. This is in qualitative agreement with the trends observed for the surface domains $(\bar{2}\,0\,3)$ and $(7\,\bar{1}\,\bar{8})$ in Figure 9; the frequency increased upon increased hydrogen pressure for $(\bar{2}\,0\,3)$, whereas the oscillations disappeared for $(7\,\bar{1}\,\bar{8})$.

Apart from E_{ox}, also the sticking probabilities typically vary for different surface structures. However, oscillations solely exist within a limited range of sticking probabilities. Within this range, the dependence of the oscillation frequency on the sticking coefficient is much weaker than the dependence on the activation energy for oxidation/reduction. Therefore, a structure-dependent sticking was not accounted for in the model used.

4. SUMMARY AND CONCLUSIONS

The present in situ PEEM observations of catalytic hydrogen oxidation on polycrystalline Rh demonstrate that under certain conditions spreading chemical waves create global oscillating spatio-temporal patterns with varying local oscillation frequency, depending on the particular surface structure. These chemical waves, generated by local surface defects, travel across grain boundaries which act as "frequency transformers" from one μm-sized Rh(hkl) domain to another. The frequency change occurs abruptly on the boundary showing a strict correlation between the frequency and the local surface structure of each particular Rh(hkl) domain. The oscillations were observed solely on stepped high-Miller-index domains, whereas smooth surfaces such as Rh(1 1 1) exhibited a usual bistable nonoscillating behavior. Formation of subsurface oxygen is suggested as the feedback mechanism of the observed oscillations. Complementary observations, such as colliding reaction fronts and existence of structural limits of the observed oscillations, experimentally corroborate this suggestion.

A microkinetic model explains the correlation between the local surface structure and the local oscillation frequency, since the subsurface oxygen formation, serving as feedback mechanism, is structure sensitive. The critical sensitivity of the oscillation frequency on the activation energy of subsurface oxygen formation explains why oscillations in H_2 oxidation were not yet observed on smooth Rh surfaces despite decades-long efforts. The absence of steps, kinks, and other low-coordinated sites hinders the formation of subsurface oxygen and prevents generation of oscillations. In contrast, on stepped and kinked Rh surfaces the more facile formation of subsurface oxygen enables self-sustained oscillations. The predicted pressure dependence of the oscillation was experimentally confirmed, further supporting the model of the feedback mechanism.

The observed new effect in hydrogen oxidation allows a direct visualization of the catalytic heterogeneity of catalytically active surfaces, opening a promising approach toward addressing the structure sensitivity of heterogeneous surfaces.

AUTHOR INFORMATION

Corresponding Author

*E-mail: guenther.rupprechter@tuwien.ac.at.

ORCID

Günther Rupprechter: 0000-0002-8040-1677

Present Address

‖Advanced Research Center for Nanolithography, Science Park 110, 1098 XG Amsterdam, The Netherlands.

Notes

The authors declare no competing financial interest.

ACKNOWLEDGMENTS

This work was supported by the Austrian Science Fund (FWF) [SFB F45 FOXSI]. H.G. acknowledges financial support from the Swedish Research Council (2016-05234).

REFERENCES

(1) Döbereiner, J. W. Propriétés nouvelles et remarquables reconnues au sus-oxide de platine, au sulphure oxidé et â la poussiere du même metal. *Ann. Chim. Phys.* **1823**, *24*, 91−96.

(2) Faraday, M. Experimental researches in electricity. Sixth series. *Philos. Trans. R. Soc. London* **1834**, *124*, 55−76.

(3) Faraday, M. *Experimental Researches in Electricity*; Taylor, R., Taylor, J. E., Eds.; Printers and Publishers to The University of London: London, 1844; Vol. 2.

(4) Berzelius, J. J. Einige Ideen über eine bei der Bildung organischer Verbindungen in der lebenden Natur wirksame, aber bisher nicht bemerkte Kraft. *Jber. Chem.* **1836**, *15*, 237−245.

(5) Norton, P. R. *The Chemical Physics of Solid Surfaces and Heterogeneous Catalysis*; King, D. A., Woodruff, D. P., Eds.; Elsevier: Amsterdam, 1982; Vol. 4, p 27.

(6) Thiel, P. A.; Madey, T. E. The interaction of water with solid surfaces: Fundamental aspects. *Surf. Sci. Rep.* **1987**, *7*, 211−385.

(7) Verheij, L. K.; Hugenschmidt, M. B. On the mechanism of the hydrogen-oxygen reaction on Pt(111). *Surf. Sci.* **1998**, *416*, 37−58.

(8) Bedürftig, K.; Völkening, S.; Wang, Y.; Wintterlin, J.; Jacobi, K.; Ertl, G. Vibrational and structural properties of OH adsorbed on Pt(111). *J. Chem. Phys.* **1999**, *111*, 11147−11154.

(9) Michaelides, A.; Hu, P. Catalytic water formation on platinum: A first-principles study. *J. Am. Chem. Soc.* **2001**, *123*, 4235−4242.

(10) Völkening, S.; Bedürftig, K.; Jacobi, K.; Wintterlin, J.; Ertl, G. Dual-path mechanism for catalytic oxidation of hydrogen on platinum surfaces. *Phys. Rev. Lett.* **1999**, *83*, 2672−2675.

(11) Sachs, C.; Hildebrand, M.; Völkening, S.; Wintterlin, J.; Ertl, G. Spatiotemporal self-organization in a surface reaction: From the atomic to the mesoscopic scale. *Science* **2001**, *293*, 1635−1638.

(12) Sachs, C.; Hildebrand, M.; Völkening, S.; Wintterlin, J.; Ertl, G. Reaction fronts in the oxidation of hydrogen on Pt(111): Scanning tunneling microscopy experiments and reaction-diffusion modeling. *J. Chem. Phys.* **2002**, *116*, 5759−5773.

(13) Mitsui, T.; Rose, M. K.; Fomin, E.; Ogletree, D. F.; Salmeron, M. A scanning tunneling microscopy study of the reaction between hydrogen and oxygen to form water on Pd(111). *J. Chem. Phys.* **2002**, *117*, 5855−5858.

DOI: 10.1021/acs.jpcc.8b11421
J. Phys. Chem. C 2019, 123, 4217−4227

(14) Wilke, S.; Natoli, V.; Cohen, M. H. Theoretical investigation of water formation on Rh and Pt Surfaces. *J. Chem. Phys.* **2000**, *112*, 9986−9995.
(15) Schaak, A.; Shaikhutdinov, S.; Imbihl, R. H/D-isotope effects in chemical wave propagation on surfaces: The O_2+H_2 and NO+H_2 reactions on Rh(110) and Rh(111). *Surf. Sci.* **1999**, *421*, 191−203.
(16) Monine, M. I.; Schaak, A.; Rubinstein, B. Y.; Imbihl, R.; Pismen, L. M. Dynamics of subsurface oxygen formation in catalytic water formation on a Rh(1 1 1) surface - experiment and simulation. *Catal. Today* **2001**, *70*, 321−330.
(17) Suchorski, Y.; Rupprechter, G. Heterogeneous surfaces as structure and particle size libraries of model catalysts. *Catal. Lett.* **2018**, *148*, 2947−2956.
(18) Beusch, H.; Fieguth, P.; Wicke, E. Thermisch und kinetisch verursachte Instabilitäten im Reaktionsverhalten einzelner Katalysatorkörner. *Chem. Ing. Tech.* **1972**, *44*, 445−451.
(19) Adlhoch, W.; Lintz, H.-G.; Weisker, T. Oszillationen der Reaktionsgeschwindigkeit bei der Reaktion von NO mit CO an Platin im Knudsengebiet. *Surf. Sci.* **1981**, *103*, 576−585.
(20) Ertl, G. Oscillatory catalytic reactions at single-crystal surfaces. *Adv. Catal.* **1990**, *37*, 213−277.
(21) Ertl, G. Reactions at surfaces: From atoms to complexity (Nobel Lecture). *Angew. Chem., Int. Ed.* **2008**, *47*, 3524−3535. ; and references therein
(22) Imbihl, R. Nonlinear dynamics on catalytic surfaces: The contribution of surface science. *Surf. Sci.* **2009**, *603*, 1671−1679.
(23) Chau, T.-D.; Visart de Bocarmé, T.; Kruse, N. Kinetic instabilities in the NO/H2 reaction on platinum. *Surf. Interface Anal.* **2004**, *36*, 528−532.
(24) Imbihl, R. Nonlinear dynamics on catalytic surfaces. *Catal. Today* **2005**, *105*, 206−222.
(25) Zuniga, J.; Luss, D. Kinetic oscillations during the isothermal oxidation of hydrogen on platinum wires. *J. Catal.* **1978**, *53*, 312−320.
(26) Rajagopalan, K.; Sheintuch, M.; Luss, D. Oscillatory states and slow activity changes during the oxidation of hydrogen by palladium. *Chem. Eng. Commun.* **1990**, *7*, 335−343.
(27) Gimzewski, J. K.; Gerber, C.; Meyer, E.; Schlittler, R. R. Observation of a chemical reaction using a micromechanical sensor. *Chem. Phys. Lett.* **1994**, *217*, 589−594.
(28) Lalik, E.; Drelinkiewicz, A.; Kosydar, R.; Szumełda, T.; Bielańska, E.; Groszek, D.; Iannetelli, A.; Groszek, M. Oscillatory behavior and anomalous heat evolution in recombination of H_2 and O_2 on Pd-based catalysts. *Ind. Eng. Chem. Res.* **2015**, *54*, 7047−7058.
(29) Li, Y.-E.; Gonzalez, R. D. Coupled oscillations of H_2/O_2/CO on silica supported rhodium catalyst. *Catal. Lett.* **1988**, *1*, 229−235.
(30) Lovis, F.; Smolinsky, T.; Locatelli, A.; Niño, M. Á.; Imbihl, R. Chemical waves and rate oscillations in the H_2 + O_2 Reaction on a bimetallic Rh(111)/Ni catalyst. *J. Phys. Chem. C* **2012**, *116*, 4083−4090.
(31) Visart de Bocarmé, T.; Bär, T.; Kruse, N. In situ dynamic study of hydrogen oxidation on rhodium. *Ultramicroscopy* **2001**, *89*, 75−82.
(32) Suchorski, Y.; Datler, M.; Bespalov, I.; Zeininger, J.; Stöger-Pollach, M.; Bernardi, J.; Grönbeck, H.; Rupprechter, G. Visualizing catalyst heterogeneity by a multifrequential oscillating reaction. *Nat. Commun.* **2018**, *9*, 600.
(33) Datler, M.; Bespalov, I.; Buhr, S.; Zeininger, J.; Stöger-Pollach, M.; Bernardi, J.; Rupprechter, G.; Suchorski, Y. Hydrogen Oxidation on Stepped Rh Surfaces: μm-Scale versus Nanoscale. *Catal. Lett.* **2016**, *146*, 1867−1874.
(34) Zaikin, A. N.; Zhabotinsky, A. M. Concentration wave propagation in two-dimensional liquid-phase self-oscillating system. *Nature* **1970**, *225*, 535−537.
(35) Imbihl, R. Oscillatory reactions on single crystal surfaces. *Prog. Surf. Sci.* **1993**, *44*, 185−343.
(36) Günther, S.; Kaulich, B.; Gregoratti, L.; Kiskinova, M. Photoelectron microscopy and applications in surface and materials science. *Prog. Surf. Sci.* **2002**, *70*, 187−260.
(37) von Oertzen, A.; Rotermund, H. H.; Nettesheim, S. Diffusion of carbon monoxide and oxygen on Pt(110): experiments performed with the PEEM. *Surf. Sci.* **1994**, *311*, 322−330.
(38) Humphreys, F. J. Review grain and subgrain characterisation by electron backscatter diffraction. *J. Mater. Sci.* **2001**, *36*, 3833−3854.
(39) Vogel, D.; Spiel, C.; Suchorski, Y.; Trinchero, A.; Schlögl, R.; Grönbeck, H.; Rupprechter, G. Local catalytic ignition during CO oxidation on low-index Pt and Pd surfaces: a combined PEEM, MS, and DFT study. *Angew. Chem., Int. Ed.* **2012**, *51*, 10041−10044.
(40) Vogel, D.; Spiel, C.; Suchorski, Y.; Urich, A.; Schlögl, R.; Grönbeck, H.; Rupprechter, G. Mapping the local reaction kinetics by PEEM: CO oxidation on individual (100)-type grains of Pt foil. *Surf. Sci.* **2011**, *605*, 23−24.
(41) Suchorski, Y.; Rupprechter, G. Local reaction kinetics by imaging. *Surf. Sci.* **2016**, *643*, 52−58.
(42) Vogel, D.; Spiel, C.; Schmid, M.; Stöger-Pollach, M.; Schlögl, R.; Suchorski, Y.; Rupprechter, G. The role of defects in the local reaction kinetics of CO oxidation on low-index Pd surfaces. *J. Phys. Chem. C* **2013**, *117*, 12054−12060.
(43) Schaak, A.; Imbihl, R. Bistability and formation of low work function areas in the O_2+H_2 reaction on a Rh(111) surface. *J. Chem. Phys.* **2000**, *113*, 9822−9829.
(44) McEwen, J.-S.; Gaspard, P.; Visart de Bocarmé, T.; Kruse, N. Oscillations and bistability in the catalytic formation of water on rhodium in high electric fields. *J. Phys. Chem. C* **2009**, *113*, 17045−17058.
(45) Suchorski, Y. Field ion and field desorption microscopy: Surface chemistry applications; *Encyclopedia of Interfacial Chemistry—Surface Science and Electrochemistry*; Wandelt, K., Ed.; Elsevier Inc.: Amsterdam, 2018; Vol. *1*, pp 162−179.
(46) Franck, U. F. Feedback Kinetics in Physicochemical Oscillators. *Ber. Bunsenges. Phys. Chem.* **1980**, *84*, 334−341.
(47) Imbihl, R.; Ertl, G. Oscillatory kinetics in heterogeneous catalysis. *Chem. Rev.* **1995**, *95*, 697−733.
(48) Yeates, R. C.; Turner, J. E.; Gellman, A. J.; Somorjai, G. A. The oscillatory behavior of the CO oxidation reaction at atmospheric pressure over platinum single crystals: Surface analysis and pressure dependent mechanisms. *Surf. Sci.* **1985**, *149*, 175−190.
(49) Suchorski, Y.; Drachsel, W.; Gorodetskii, V. V.; Medvedev, V. K.; Weiss, H. Lifted reconstruction as a feedback mechanism in the oscillating CO oxidation on Pt nanofacets: Microscopic evidences. *Surf. Sci.* **2006**, *600*, 1579−1585.
(50) Rotermund, H. H.; Lauterbach, J.; Haas, G. The formation of subsurface oxygen on Pt(100). *Appl. Phys. A* **1993**, *57*, 507−511.
(51) von Oertzen, A.; Mikhailov, A.; Rotermund, H.-H.; Ertl, G. Subsurface oxygen formation on the Pt(110) surface: experiment and mathematical modeling. *Surf. Sci.* **1996**, *350*, 259−270.
(52) Schaak, A.; Imbihl, R. Spiral waves and formation of low work function areas in catalytic NO reduction with hydrogen on a Rh(111) surface. *J. Chem. Phys.* **2002**, *116*, 9021−9027.
(53) Badan, C.; Farber, R. G.; Heyrich, Y.; Koper, M. T. M.; Killelea, D. R.; Juurlink, L. B. F. Step-type selective oxidation of platinum surfaces. *J. Phys. Chem. C* **2016**, *120*, 22927−22935.
(54) Farber, R. G.; Turano, M. E.; Oskorep, E. C. N.; Wands, N. T.; Juurlink, L. B. F.; Killelea, D. R. Exposure of Pt(5 5 3) and Rh(1 1 1) to atomic and molecular oxygen: Do defects enhance subsurface oxygen formation? *J. Phys.: Condens. Matter* **2017**, *29*, 164002.
(55) Wider, J.; Greber, T.; Wetli, E.; Kreutz, T. J.; Schwaller, P.; Osterwalder, J. Direct observation of subsurface oxygen on Rh(111). *Surf. Sci.* **1998**, *417*, 301−310.
(56) Zum Mallen, M. P.; Williams, W. R.; Schmidt, L. D. Steps in hydrogen oxidation on rhodium: hydroxyl desorption at high temperatures. *J. Phys. Chem.* **1993**, *97*, 625−632. ; and references therein
(57) McEwen, J.-S.; Gaspard, P.; de Bocarme, T. V.; Kruse, N. Nanometric chemical clocks. *Proc. Natl. Acad. Sci. U.S.A.* **2009**, *106*, 3006−3010. ; and Supporting Information therein

DOI: 10.1021/acs.jpcc.8b11421
J. Phys. Chem. C 2019, 123, 4217−4227

(58) Gregoratti, L.; Baraldi, A.; Dhanak, V. R.; Comelli, G.; Kiskinova, M.; Rosei, R. Structural effects on water formation from coadsorbed H + O on Rh(100). *Surf. Sci.* **1995**, *340*, 205−214.
(59) Klikovits, J.; Schmid, M.; Merte, L. R.; Varga, P.; Westerström, R.; Resta, A.; Andersen, J. N.; Gustafson, J.; Mikkelsen, A.; Lundgren, E.; Mittendorfer, F.; Kresse, G. Step-orientation-dependent oxidation: From 1D to 2D oxides. *Phys. Rev. Lett.* **2008**, *101*, 266104.

DOI: 10.1021/acs.jpcc.8b11421
J. Phys. Chem. C 2019, 123, 4217−4227